



زانكۆی سه‌لاحه‌دین- هه‌ولێر

Salahaddin University-Erbil

Active eclipsing binary RT Andromedae revisited

By:

Dunya Muhammad Kakil

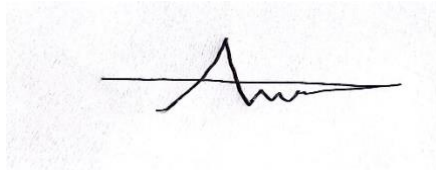
Supervised By:

Dr.Aven Magded Hamadamen

April-2024

This research project has been written under my supervision and has been submitted for the award of the degree of B.Sc. in (Physics)

Supervisor:



Signature:

Name: Dr. Aven Magded Hamadamen

Date: /4/2023

I confirm that all requirements have been completed.

Signature:

Name: Dunya Muahammad

Head of the Department of Physics

Date: / 4/ 2023

Acknowledgement

*I am so thankful to my supervisor **Dr. Aven Maghded**, It is an honor for me to have completed my research under the supervision of Dr. Aven ,he really helped me a lot and he was so tired with me from the beginning, And I'm also very grateful to my friend **Helin Jawhar**, who was a great contributor to my research.*

Dunya

Content

<i>Abstract</i>	5
<i>Chapter one</i>	6
1. Introduction.....	6
1.1. Binary Stars	6
1.2. Type of Binary Stars	8
1.3. Classification of Binary Stars	9
1.3.1. Optical double.....	9
1.3.2. Visual Binaries.....	9
1.3.3. Astrometric Binaries.....	10
1.3.4 Spectroscopic Binaries	11
1.3.5. Eclipsing Binaries	12
2. Methods	16
<i>Chapter Two</i>	18
2.3. Atmospheric Parameters	21
2.4.Absolute Parameters	22
2.4.8. Surface Potential	25
2.4.9. Equipotential Surfaces	26
2.4.13. Gravity Brightening	26
2.4.14. Reflection coefficients	27
2.4.15. Luminosity.....	27
<i>Chapter Three</i>	28
3. RT Andromeda	28
3.1. The orbital period analysis	29
4. The Life Time	34
5. Results and discussion	37
6.Reference	37

Abstract.

The photometric and spectroscopic data of the short-period RS CVn-like binary RT And have undergone a consistent reanalysis. Explanations for the long-term change in orbital period include two-period leaps, a continuous period decrease combined with the light-time orbit, or two light-time orbits. Without maculation effects, B, V, and R filters light curves and the radial velocities of both components were analyzed with the Wilson-Devinney program to compute the photometric and spectroscopic elements and deduce the masses of the components: $m_1 = 1.100.02 M_{\odot}$ and $m_2 = 0.830.02 M_{\odot}$. Photoelectric observations of the secondary minimum confirmed the high orbital inclination $i = 87.6 \pm 0.1$. During the secondary minimum, the average observed U light curve reveals additional light. It cannot be ruled out that the light-curve analysis revealed a minor eccentricity, as discovered by multiple authors. The proximity of the marks on the surfaces of both components in 1971 suggests the possibility of mass transfer from the primary to the secondary component via a magnetic bridge connecting both active regions. Analysis of all available light curves suggests a random distribution of star spotting and does not corroborate the existence of active longitude belts. The distance of RT And is calculated to be 832 pc, which is near the Hipparcos value of 756 pc based on the absolute parameters of the binary and the maximum apparent V brightness.

Key words: stars: binaries: eclipsing – stars: individual: RT

And – stars: magnetic fields

Chapter One

Introduction

1.1 Binary Stars

The term binary was first used in this context by Sir William Herschel in 1800 (AD)(applegate,J.H,1992) . Binary stars, often called double stars, refer to pairs of stars sufficiently close to each other in space to be gravitationally bound together, orbiting around common center of mass gravitationally bound to each other formed at the same time as has been illustrated in the Fig. (1-1). The two members of a binary star are of unequal brightness (M, et al.2009). The brighter star is called the primary and the fainter is called the companion (T and T,1996). Binary systems are of special interest, because analysis of their orbital characteristics is done by using of Kepler's third law which yields a direct measure of stellar masses(Briede,A.1949). Binary stars which can be resolved with a telescope or inter ferometric methods are known as visual binaries. Most of the known visual binary stars have not completed one whole revolution, but are observed to have travelled along a curved path or a partial arc. At least 80% of all stars in the Milky Way are part of multiple systems (binaries, triplets or more) some are close enough that they are able to transfer matter through tidal forces. These are close or contact binaries according to conservative statistics. There seems to be no obvious preference for particular combinations of brightness, size, or mass differences and a wide range in periods of revolution from less than a day to thousands of years. Likewise, there is a large range in separations from those stars in contact to those separated by thousands of times the Earth to Sun distance. Historically, visual binaries are which those that appear as double stars when seen through a telescope, were discovered to be

gravitationally bound by William Herschel around 1800(AD)
 (Applegate,J.H.1992).

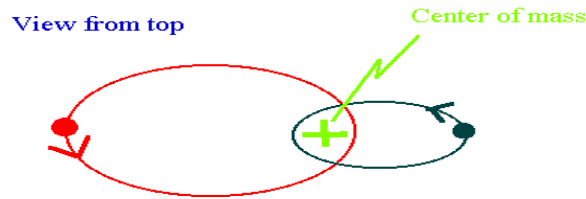


Figure (1-1): Binary stars orbiting their center of gravity (Budding,E.1984.)

It is noticeable from the Fig. (1-1) that the orbits of two stars of a binary system, relative to the center of mass of the two stars. The more massive star M has a smaller orbit than the less massive star m, but both orbit with the center of mass at one focus of their ellipses. While the Fig. (1-1), shows that the system can be considered equally well as one star (the secondary) orbiting the other (the primary). The dashed line represents the distance between the two stars at a particular moment in time as shown in the above figure, with the same length and direction, to aid in relating the two equivalent ways of visualizing the geometry but it can be considered that one star fixed, with the other star orbiting in a larger ellipse.. These Binary systems are important astrophysical laboratories because they allow us to deduce the properties of the constituent stars more concretely than we can with single stars. The physics that governs how stars orbit one another was developed by Newton and Kepler over three hundred years ago, and can be summarized by the equation.

$$P^2 = \frac{4\pi^2}{G(M_p+M_s)} a^3 \dots\dots\dots(1-1)$$

Where G is the gravitational constants and M_p and M_s are the masses of the two components (a) is the semi-major axes of the two orbits $a = a_p + a_s$

In cmgs units , $G=6.67 \cdot 10^{-11} \text{ dyn cm}^2 \text{ g}^{-2}$ but these units are not the units of choice, Where mases measured in solar masses distances in AU⁽¹¹⁾.

1.2 Types of Binary Stars:

For decades, the study of eclipsing variable stars formed an important branch of variable stars or systems as shown in Fig. (1.2) which shows the flow chart for outline scheme of Photometric classification of eclipsing variables and its successive criteria .The most important of the two branches related to eclipsing variables is the branch of binary systems .The problem of binary system classification has come over a wide range of effecting parameters on which or accordingly, the related identification to a certain class is drawn. Both wide and close binary systems have subdivision groups depending on the dominant parameter taken as major factor of classification. It has been found that the majority of eclipsing variable, which are among the most useful representatives of this field are" close " binary system. Increased attention to such system is due to the behavior of their light variation, therefore, it has been customary for many years to divide eclipsing variables into the following groups. This classification includes the following types Kopal (1959):

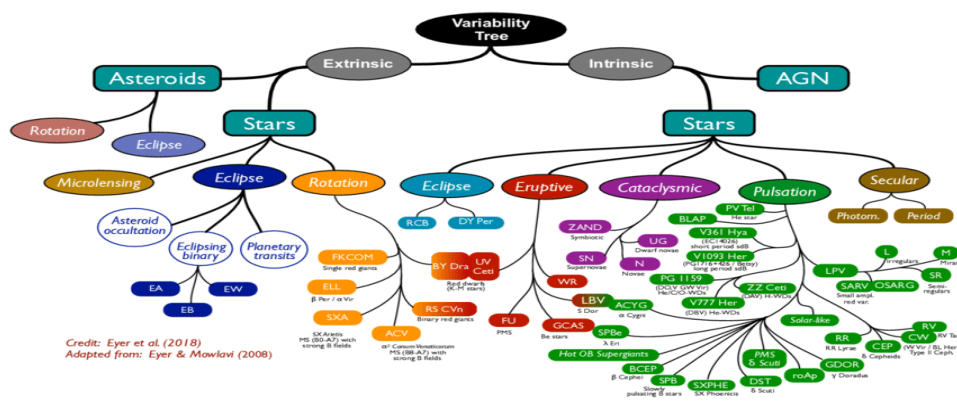


Figure (1-2): Binary stars tree.

1. 3 Classifications of Binary Stars by Methods of Observation:

Binary stars are classified into four types according to the way in which they were observed: visually, by observation; spectroscopically, by periodic changes in spectral lines; photometrically, by changes in brightness caused by an eclipse; or astrometrically, by measuring a deviation in a star's position. Any binary star can belong to several of these classes; for example, several spectroscopic binaries are also eclipsing binaries.

1.3.1 Optical Double

This is not really a binary star. Two stars just happen to appear along almost the same line of sight. The two stars appear very close in the sky but are at different distances from Earth. They are actually very far apart (Pands.2018). The two objects are totally unrelated and are actually moving through space at right angles to each other. They passed at a minimum separation of 9 seconds of arc in 1960 and have been separating ever since (G and F.1981).

1.3.2 Visual Binaries

True binary star systems (as opposed to purely optical doubles) in which both components are visible and resolvable in a telescopic eyepiece, Astronomers consider a visual binary, assuming initially that the brighter primary component is stationary and the fainter secondary component is orbiting around it (P and R.1927). The angular separation of the stars and the angular direction to the secondary can be directly observed. Making use of observations extending over many years or decades, the relative orbit of the secondary can be determined. In most cases, the two stars components differ in brightness (G, et al.1975). The first binary orbit to be determined was that of W UMa in 1830 as shown in figure (1-3). With the

current generation of stellar interferometers, many more binary systems fall into this category, although some researchers call these “interferometric binaries”. Knowledge of the positions of the stars on the sky, as a function of orbital phase, coupled with RV observations; allow the masses of the stars to be measured directly, along with their luminosity ratio. These stars are therefore good for determining the mass–luminosity relation of stars, but, more importantly, they provide an essentially geometric determination of the distance to the system which is very reliable.

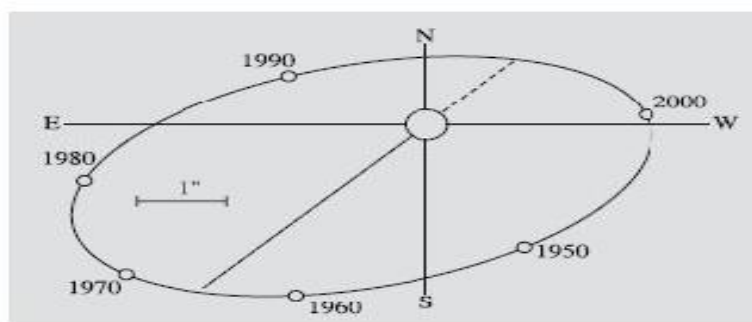


Figure (1-3): The orbit of M Ursae Majoris was the first binary orbit determined observationally in 1830(H, et al.1953)

1.3.3 Astrometric Binaries

If only one component is visible, because the other is too faint and/or is too close to its brighter companion to be separated through telescopic resolution alone, gravitational effects may help one to prove that the system is a binary. The first astrometric binary was Sirius, which in the 1830’s was observed to have an undulating proper motion. It was concluded that it had a small companion, which was visually discovered a few decades later, see Figure (1-4). The companion, Sirius B, was a completely new type of object, a white dwarf the proper motions of nearby stars have been carefully studied in the search for planetary systems. Although for example Barnard’s star may have unseen companions, the existence of planetary

systems around other O stars was not established by proper motion studies but with spectroscopic observations (Puget and Heyvaerts.1980). Another interesting type of astrometric binary is presented by cases where the components are so close that they are, or have been until recently, irresolvable. Fig: (1-4) shows the proper motion of the Sirius system over 70 years, the slight perturbations or wobble in the bright star, Sirius A, is due to the presence of its much dimmer white dwarf companion, Sirius B (Kopal,Z.1959).

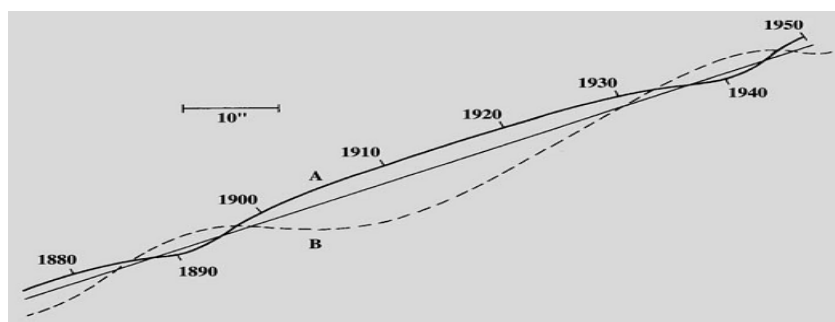


Figure (1-4): The apparent paths of Sirius and its companion in the sky .(H,et al.1953)

1.3.4 Spectroscopic Binaries

Spectroscopic binary systems are those for which their binarity is apparent from variation of their radial velocity. The secondary component may also produce spectral lines strong enough to be visible in the spectrum of the system, in which the case of the spectroscopic binary is “double-lined”. Spectroscopic observations of these systems allows calculation of the orbital period and eccentricity, the mass ratio, and the minimum masses of the components, $M \sin 3i$, where i is the inclination of the orbit relative to the line of sight of the observer. Spectroscopic binaries have too small separation for the components to be seen individually, but the binary nature of the system betrays itself because of the Doppler shifts in the spectrum (Kopal Z.1979). This causes the absorption line to be displaced toward the

blue end of the spectrum as the primary approaches the Earth in its orbit, and then to the red end as it recedes (H, et al.1953).The first to be discovered was the brightness star of the double star Mizar, which was itself shown to be a binary in 1889 by E. Pickering (Kopal,Z.1953). If the stars are moving across our line of sight then no Doppler shifting occurs so the lines stay in their mean positions. As the stars continue orbiting, A will recede so its spectral lines will move towards the red end of the spectrum and B's will move toward the blue.This is shown schematically in figure (1-5).

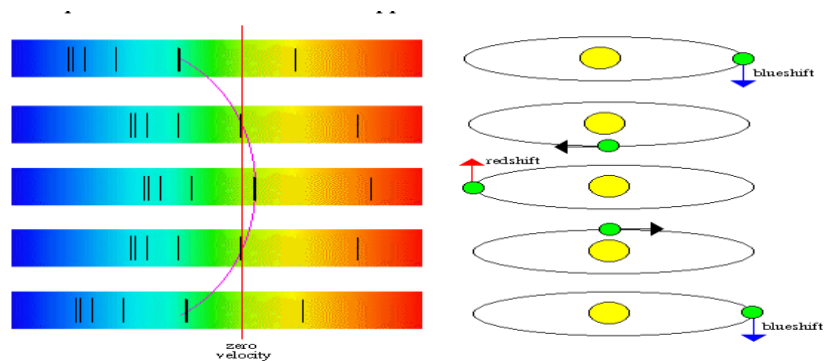


Figure (1-5): Spectroscopic binary star from APOD.

1.3.5 Eclipsing Binaries

Eclipsing Binaries are those binary systems in which the orbital plane of the system is almost side on as seen from the Earth so that as the stars move around the common center of gravity there are eclipses. Stars in an eclipsing binary system are usually so close together that they cannot be separated even in the most powerful telescopes and are usually called eclipsing variables (Kopal z.1979). They are in an eclipsing system because of the way the light from the system varies in a regular and characteristic pattern. An eclipsing binary allows scientists to find out a lot about how binary systems evolve and thus the fate of most stars. A primary eclipse occurs when the brighter star is eclipsed by the fainter star. The secondary eclipse occurs when the fainter star is eclipsed by the brighter

star. Assuming the two stars are of the same brightness then both eclipses will be equal. If one of the stars is much fainter than the other the secondary eclipse may not be readily observed by visual observers. If the orbits of the two stars are circular then the secondary eclipse will occur midway between primary eclipses. Suppose that the orbits are elliptical the secondary eclipse may occur earlier or later than midway. There can also be a prolonged period of minimum light with an annular eclipse Figure (1-6) shows the Schematic picture of a simple eclipsing binary, and its light curve. In the light curve, time increases to the right, as the smaller, brighter star (in black in this diagram) passes in front of the larger, fainter star (left), there is a secondary minimum. t_1 , t_2 , t_3 , and t_4 are the times of the four contacts. As the brighter star passes behind the fainter one (right), there is a primary minimum (Koch, et al.1970)

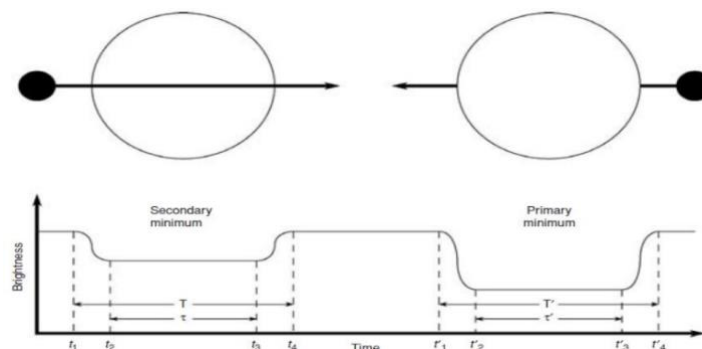


Figure (1-6): Schematic picture of a simple eclipsing binary, and its light curve.(J.M, et al.2001)

1.4 Types of Eclipsing Binaries

There are three basic types of eclipsing binary which are classified according to the shape of their light curves. The light curve will be the observed magnitudes over the whole period of the system; these types are (Wands,2009).

1.4.1 Algol Stars

The Algol-type eclipsing variables have been named after β Persei or Algol . During most of the period, the light curve is fairly constant. This corresponds to phases during which the stars are seen separate from each other and the total magnitude remains constant. There are two different minima in the light curve, one of which, the primary minimum, is usually much deeper than the other one. This is due to the brightness difference of the stars. When the larger star, which is usually a cool giant, eclipses the smaller and hotter component, there is a deep minimum in the light curve. When the small, brighter star passes across the disc of the giant, the total magnitude of the system does not change by much (H, et al.1953) . The light curve of Algol shows a significant difference in the depths of their two minima . The shape of the minima depends on whether the eclipses are partial or total. In a partial eclipse the light curve is smooth, since the brightness changes smoothly as the depth of the eclipse varies. In a total eclipse there is an interval during which one component is completely invisible. The total brightness is then constant and the light curve has a flat bottomed minimum. The shape of the minima in Algol variables thus gives information on the inclination of the orbit. Figure (1-7) shows the light curve of Algol type(Koch,et al.1970). The duration of the minima depends on the ratio of the stellar radii to the size of the orbit. If the star is also a spectroscopic binary, the true dimensions of the orbit can be obtained. In that case, the masses and the size of the orbit, and thus also the radii can be determined without having to know the distance of the system (Wands,2009) .

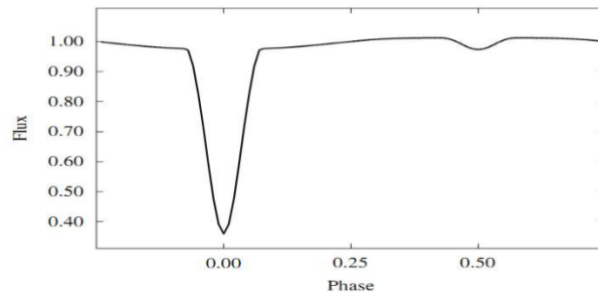


Figure (1-7): Synthetic " Algol "type light curve (V band) (Koch, et al .1970)

1.4.2 β Lyrae Stars

In the β Lyrae-type binaries, the total magnitude varies continuously. The stars are so close to each other that one of them has been pulled into ellipsoidal shape. Thus the brightness varies also outside the eclipses. The β Lyrae variables can be described as eclipsing ellipsoidal variables. In the β Lyrae system itself, one star has overfilled its Roche lobe and is steadily losing mass to its companion. The mass transfer causes additional features in the light curve (Zasche and p,2011). Figure (1-8) shows synthetic β Lyrae type light curve (Wands,2009) and (A,et al.2012). The orbital period is in general greater than one day .In addition, β Lyrae type stars has many features which can be summarized as follows:

1-It is continuously variable.

2-It has quiet difference in surface brightness.

3-It has large difference in minima depths (Matteucci and franceca,2001)

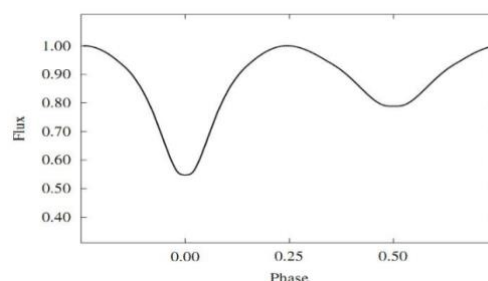


Figure (1-8): Synthetic β Lyrae type light curve (V band) (Wands,2009) and (A,et al,2012)

2. Methods

Our method of detection and characterization of the sample binaries uses a classical approach assuming only one body on a quite distant orbit, meaning there is no dynamical interaction, and only the LITE term was used for ETV analysis. With this method, we would be able to find preferably the bodies with periods of a few years to decades, and with LITE semiamplitudes of the order of 0.01 day (quite similarly to our former analysis, (Zasche et al. 2014)). This limitation mainly comes from the fact that the data cadence is typically limited, and the precision of the individual times of eclipses critically depends on the quality of the light curve (LC) and depth of a particular eclipse. The PDR code (Zejda et al. 2019) was used to obtain some of these data. These datasets were the following:

* HIP: the Hipparcos satellite, observing in special Hp filter, between 1989 and 1993 (Perryman et al. 1997).

*NSVS: the ROTSE-I experiment, unfiltered photometry, with a time span from 1999 to 2000 (Wozniak et al. 2004).

*OMC: five-cm camera onboard the INTEGRAL satellite, observing in V filter since 2002 (Mas-Hesse et al. 2003).

* ASAS: All Sky Automated Survey, observing since 1997 in V and I filters (Pojmanski 2002).

*ASAS-SN: ASAS for supernovae, 24 telescopes, V and g filters (Shappee et al. 2014; Kochanek et al. 2017).

– SuperWASP: 20-cm telescopes, using special filters, observing since 2004 (Pollacco et al. 2006).

- Pi of the sky: small robotic cameras, observing since 2004, unfiltered (Burd et al. 2005).
- CRTS: Catalina Survey, 70-cm telescope, observing since 2007, unfiltered (Drake et al. 2009).
- Kepler: Kepler satellite, 95-cm telescope, observed from 2009 to 2018 in special filter (Borucki et al. 2010).
- TESS: TESS satellite, 10-cm diameter, observing since 2018 in special filter (Ricker et al. 2015).
- KWS: Kamogata/Kiso/Kyoto wide-field survey, observing in BV Ic filters (Maehara 2014).
- MASCARA: small 17-mm wide-field cameras, observing since 2017, unfiltered (Burggraaff et al. 2018).
- ZTF: the Zwicky Transient Facility, 120-cm telescope, g, and r filters (Masci et al. 2019).

For the derivation of times of mid-eclipse, our automatic fitting procedure (AFP, Zasche et al. 2014) was used. It uses an LC template and phased LCs at particular time intervals when the phase coverage of both minima is sufficient. Therefore, the cadency of these derived minima highly depends on the particular survey, its cadency, and the precision of individual photometric data points. For the systems where no previous LC solution exists, we also performed an LC analysis. This was typically based on the best available LC for that particular system, meaning from the source (from the aforementioned list) that provides the best phase coverage as well as the lowest scatter of the individual observations. The individual cases are discussed in more detail below.

Chapter Two

Modeling light Curves Theory of Algol Binary Stars

2.1 An Over View of Light Curve

In the present work author makes use of this type of photometrical observation which have been sent to her by private communication. Significant progress of computational astrophysics was made in the early 1970s. Models and programs were developed to compute (synthetic) light and velocity curves directly. Such models and programs were based on spherical stars, treated in the Eclipsing Binary Orbit Program (EBOP) [Nelson & Davis 1972; ellipsoidal geometry, treated in WINK program developed by Wood 1971. Lucy 1968, Wilson & Devinney 1971, produced models and programs based on Roche geometry's". FORTRAN program EBOP is based on the Nelson & Davis 1972 spheroidal model called the NDE model. It is an efficient software for the analysis of detached binary systems with minimal shape distortion due to proximity effects. The NDE model and its assumptions are close to those in the rectification model by (Matteucci and Franceca, 2001). EBOP makes use of spheroidal stars moving in circular or eccentric orbits. The Wood 1972 WINK program is based on the Wood 1971 model. The model assumes the components of the binary system to be tri-axial ellipsoids. Physic_&_ models based on equipotential and Roche geometry are implemented in the Wilson-Devinney program, used in present work for W UMa type of eclipsing binary star. A breakthrough occurred with the introduction of Roche geometry. An example of improved astrophysical understanding through eclipsing binary light curve analysis is the successful modeling of W UMa stars as over-contact systems (Rucinski, S.M. 1966). The history of the study of eclipsing

systems of later spectral classes such as W UMa goes back to the beginning of the (Wood,1972) This class of contact systems of the close binary stars is the most numerous and has been most observed photometrically and spectroscopically. This is because of their short periods and the procedure for identifying them as eclipsing variables.

2.2 Wilson and Devinney Program:

The Wilson-Devinney program is the most widely used of all the synthetic and analytic light curve modeling codes in photometry of spectroscopy studies . It is appropriate to describe its features, capabilities, and continuing developments in some detail. It has seen continual improvements and the current version 2006 with its powerful features provides the opportunity to extract a maximum of information from a variety of observational data (M,Cameron,L.1985).The stand-alone Fortran77 program WD 2006 enables the user to make use of the Wilson- Devinney (WD) program to compute the parameters of eclipsing binary light and radial velocity curves and to analyze observational data, i.e., to fit light curves or merely to compute a synthetic light curve(Matteucci and franceca,2001). The overall program consists of two parts of FORTRAN program designed especially for the analysis of binary star data: one is LC (Light Curve generation) in which observers input data the star parameters and the program then calculates the light curves and/or radial velocity (RV) curves that observers should observe. The other is DC (Differential Corrections) in which the program takes observers data and calculates the corrections that astronomers need to make to the basic parameters in order to improve the fit (Matteucci and franceca,2001). The WD model provides several modes to specify the geometry of the binary system or to add constraints or relations between parameters. The

WD modes are summarized as follows:

Mode-1: This mode is for X-ray binaries for which the eclipse duration of a compact object is known from X-ray observations.

Mode0: No constraints are applied in mode 0, and the component luminosity ratio is not even required to be consistent with the surface temperatures. This mode is the closest analogue to the Russell model.

Mode1: This is a mode for over-contact binaries, such as WUMa system ($T_1=T_2$ common envelope)

Mode2: This is for detached binaries with no constraints' on the Roche potential (surface potentials).

Mode3: This is for over-contact binaries and is the same as mode 1, except that the constraint on T_2 is not applied. In the present work, only this mode have been used for the present investigation.

Mode4: This is for semi-detached binaries with star 1 accurately filling its limiting lobe, which is the classical Roche lobe for synchronous rotation and a circular orbit, but it is different from the Roche lobe for non-synchronous rotation and eccentric orbits.

Mode5: The same as mode4, except that it is star2 that fills its limiting lobe. This is the usual mode for Algol type binaries.

Mode6: This is for double contact binaries.

LD: This sets the limb darkening law. LD = 1 for the linear cosine law, LD = 2 for a logarithmic law. The complete logarithmic law is: (Wands, 2009)

$$I / I_0 = 1 - x + x \cos \beta - y \cos \beta \ln(\cos \beta) \quad (2-1)$$

If $LD = 3$, the bolometric square root law is used in this work. The complete square root law is: (Wands, 2009)

$$I / I_0 = 1 - x + x \cos \beta - y(1 - \sqrt{\cos \beta}) \quad (2-2)$$

JDPHS: This is 1, if the independent variable is time and 2 if it is phase. Where β : is the angle measured between observer line of sight and the surface normal of a particular surface area element. x : limb darkening coefficient, y : bolometric limb darkening coefficient, I : intensity. The input parameters are given in appendix (paschke,1997)

2.3 Atmospheric Parameters.

Generally, stellar atmospheres have non-uniform surface brightness, this fact is exaggerated when a star fills its Roche lobe and takes on a distorted shape. The two main phenomena that act to alter the surface brightness of a star are limb darkening and gravity darkening. If star spots are present, they will affect the appearance of the star and light curve too. Finally, if there is another source of light in the system which shines onto a portion of the star, the bolometric albedo of the star will determine how much of the light is reflected back and seen by the observer. All of these phenomena work together to give the Roche lobe-filling star a non-uniform brightness, and hence, affect the shape of the observed light curves (S.B,et al.2000). Therefore, the computation of the flux emitted by the stellar photosphere based on several assumptions about the underlying photosphere physics. These include the choice of a model atmosphere and several effects: gravity darkening, limb-darkening, reflection effect and the Stellar spot (H,et al 2007)

2.4 Absolute Parameters:

The most of astronomers knowledge of absolute parameters of stars beyond the sun have been derived from the study of binary star system, and most especially of individual eclipsing photometric. A mathematical analysis of the light curves enables one not only to determine the physical and geometrical elements of selected binary systems but also to find their absolute parameters. In order to calculate the absolute parameters of the binary system the following formulae have been used (paczynki,B.1971) and (S.B, et al.2000).

$$A^3 = 74.5 p^2 (M_1 + M_2) \text{ ----- (2-17)}$$

$$(M_2/M) = q (M_1/M) \text{ -----(2-18)}$$

$$R_1 = Ar_1, R_2 = Ar_2 \text{ ----- (2-19)}$$

$$L_1 = R_1^2 T_1^4, L_2 = R_2^2 T_2^4 \text{ ----- (2-20)}$$

$$M_1 = \frac{1}{1+q} M, M_2 = \frac{q}{1+q} M \text{ -----(2-21)}$$

Where equation (2-17) is Kepler's third law, A is the separation between the two components expressed in solar radii, P is the orbital period in day, M_1 and M_2 are the masses of the components in solar mass. Equation (2-18) is the relation between masses for the primary components to the secondary one, q is the mass ratio. Equation (2-19) is the relation between absolute R_1 and R_2 , and relative r_1 and r_2 are radii of the components. The relative radii have been taken equal to the geometrical mean of the polar, side, and back radii, that were computed in this work for all selected binaries with (W-D) program. Equation (2-20) is the Stefan-Boltzmann law, L_1 and L_2 are bolometric luminosities expressed in solar units, T_1 and T_2 are the effective temperature in units of solar effective temperature.

The Table (3-7) represent the present work comparison with other workers.

2.4.1 Mass Ratio (Q)

The mass ratio q is usually defined as the mass of the less massive star (M_2) divided by that of the more massive star (M_1) (Rucinki,S.M.1966).

$$Q=M_2/M_1 \quad (2-22)$$

2.4.2 The Radii - R :

The following formula was used for determining the absolute radii determinations of both components in each system (Wood,D.B.1972)

$$R_{1,2}/R_{sun} = ar_{1,2} \quad (2-23)$$

Where a is the separation of the two components in solar units R_{sun} .

2.4.3 Bolometric Magnitudes- $M_{bol(1,2)}$:

These parameters can be evaluated using the relation given by (Whitney,B.S.1957) and (Liakose,et al.2009)

$$M_{bol(1,2)} = 42.36 - \log T_{1,2} - 5 \log(R_{1,2}/R_o) \quad (2-24)$$

Where all parameters have the same mentioned meanings.

2.4.4 Age- Mass relationship for CA binaries of stars:

More recently relationship between stellar masses and ages have been used of the form given by Barrado et al (1994).(Matteucci and franceca,2001)

$$\text{Log(Age)} = 9.883 - 2.965 \log \left[\frac{M}{M_o} \right] \quad (2-25)$$

This relation is very close to that for stars on the TAMS, which was fitted for different luminosity classes. There is a good agreement between the estimates of the ages for the two components of a given system with literature, which proves that the more reliability of this relation. Table (3-9) represent the stars and some relevant stellar parameters, these new analyses serve the basis for new calculation values for the components ages.

2.4.5 The Life Time.

This life time has been for the short period binary systems from the famous mass-luminosity relation and the results are presented in the Table (3-10).

$$\frac{t_{1,2}}{t_0} = \frac{1}{(M_{1,2}/M_0)^{2.5}} \quad \dots (2-26)$$

2.4.6 First Contact Angle:

The first contact angle (θ_1) can be derived from the following equation

$$\theta_1 = \sin^{-1} \sqrt{(r_1+r_2)^2 \csc^2 i - \cot^2 i} \quad \dots (2-27)$$

$$a = r_1 / (r_1+r_2) \quad \dots (2-28)$$

$$c = \cos i / (r_1+r_2) \quad \dots (2-29)$$

r_1 and r_2 denote the fraction radii and (i) the inclination of the orbital plane to the celestial sphere . The eclipse is bound to be partial if: $1 > c_0 > |2a-1|$, While it becomes total if $c_0 < 1-2a$, by applying the above formula to all stars under investigation we found that for about some values of them is not correct and give different type of the eclipse. Also (whitney,B.S.1957) has mentioned that the theoretical value of the first contact angle is less than 55° for all type of eclipse. However (H, et al,2007) found that G_1 , for Algol vary from 23° to 30° while its value for W Uma-type system vary

from 40° to 49° Jabbar (1983) .The results for the systems are given in Table (3-12).

2.4.7 Empirical Relationship between CI , M_{bol} and T_{eff} :

Specifically bolometric correction is defined to be the number of magnitudes that must be added to absolute visual magnitude (M_v) to give absolute bolometric magnitude (M_{bol}), $M_{bol} = M_v + BC (T)$. The definition above was used since solar-like stars have their radiation maximum in the visual region of the spectrum, and due to the definition of the zero point of B.C. , most stars have negative bolometric correction. Some care is necessary in the use of B.C. from tables because sometimes the definition, $B.C. = M_v - M_{bol}$ is used as given by (Paczynski, B.1971):

Where B.C.: is the bolometric correction has been tabulated as a function of spectral type and (B-V) index.

$$M_{sun} = 4.83$$

$$B.C._{sun} = -0.07$$

$$B-V = -3.684 \log (T) + 14.551 \quad \dots (2-30)$$

For $\log (T) < 3.961$

$$B-V = 0.344[\log (T)]^2 - 3.402 \log(T) + 8.037 \quad (2-31)$$

For $\log (T) > 3.961$

$$BC = -8.499[\log(T)-4]^4 + 13.421[\log(T)-4]^3 - 8.131[\log (T)-4]^2 - 3.901[\log(T)-4] - 0.438 \quad (2-32)$$

Where BC represents bolometric correction and CI denotes color index. While the Table (3-13) represents the empirical values for the present work.

2.4.8 Surface Potential (Ω)

The Surface Potential Ω , along with a specified mass ratio, completely describes the surface structure for synchronously rotating,

circular orbit binary stars. It takes into account both the gravitational and centrifugal forces in the binary. As the value of the surface Potential is increased, the size of the star decreases. This makes sense since the gravitational potential increases as one approach the mass center. Ω is the value of the outer critical Roche equipotential and represents the limit to stability to any over contact system since the outer potential has a "hole" in it (gravitational acceleration = 0) and gas will leave the system (Rucinski,S.M.1966).

2.4.9 Equipotential Surfaces (C)

Some workers (Mochacki & Doughty 1972; Binnendijk 1977) use this parameter instead of Ω to parameterize the equipotential surfaces. The following relations relate it to Ω is (Wood,D.B.1972)

$$C=2B_1\Omega \pm 2B_2^2 \quad \dots (2-33)$$

Where $B=1/1+q$

$$B_2=q/1+q \quad \dots (2-34)$$

2.4.13 Gravity Brightening (Darkening) Exponent

By proved that for totally radiative stars the surface flux was directly proportional to the value of the gravitational acceleration (g) at the stellar surface. (The gravitational acceleration is $\nabla\Omega$) (Liakos,et al.2009)The gravity-darkening coefficients were determined by black body radiation spectrum as:

$$g_{1,2} = \frac{c_2}{4\lambda T_{1,2}[1-\exp(-c^2/\lambda T_{1,2})]} \quad \dots (2-35)$$

Where c_2 is equal to $\frac{1.43883}{(\lambda T_{1,2})_{eff}}$ and λ_{eff} is effective wavelength for used filter.

2.4.14 Reflection coefficients:

The reflection coefficients were evaluated the following equations.

$$E_{\text{eff1}} = t_1 \left[\frac{T_2}{T_1} \right]^4 \frac{e^{(c_2/\lambda T_2 - 1)}}{e^{(c_2/\lambda T_1 - 1)}} \quad (2-36)$$

$$E_{\text{eff2}} = t_2 \left[\frac{T_1}{T_2} \right]^4 \frac{e^{(c_2/\lambda T_1 - 1)}}{e^{(c_2/\lambda T_2 - 1)}} \quad (2-37)$$

2.4.15 Luminosity (wavelength dependent)

The luminosity of a star is a measure of its total output energy. Luminosities L_1 and L_2 that indicate the percentage of the total luminosity each star emits. The total luminosity is normalized to 1.00, so that $L_1 + L_2 = 1$. These quantities are wavelength dependent (H, et al.2007). The parameters were evaluated for each component by using the well-known relation Stefan Boltzman law (Paczynski, B.1971)

$$L_{1,2} = \left(\frac{R_{1,2}}{R_o} \right)^2 \left(\frac{T_{1,2}}{T_o} \right)^4 \quad (2-38)$$

Where $T_o = 5770$ K is the Sun's effective temperature (Allen (1976) (Liakoe, et al.2009), and R_1, R_2 are radius of primary and secondary stars respectively, L_1 and L_2 , the luminosities of the components in solar units L_o . While T_1 and T_2 are the temperatures of the components.

Chapter Three

Results and Discussion

3. RT Andromeda

Active eclipsing binary RT And (BD +52_3383a, F8-G0 V + K1-3V, $V_{\max} - 8.9$) is RS CVn-like short-period ($P = 0.62893$ days) system. The variability of RT And has been known since the beginning of the 20th century (Deichmueller, 1901; Zinner, 1915). The photographic light curve (LC) of RT And was obtained by Jordan (1929) and later by Payne-Gaposchkin (1946). The first photoelectric LCs of RT And were obtained in 1948 – 1950 by Gordon (1948, 1955). She found the LC to be variable and asymmetric in the secondary eclipse and noted that the primary minima occurred earlier than predicted. Wood & Forbes (1963) fitted the observed period decrease using the third order polynomial. Williamson (1974) interpreted the observed orbital period decrease by two period jumps caused by instantaneous mass exchange bursts. On the other hand, Albayrak et al. (1999) and Borkovits & Hegedűs (1996) explained the long-term orbital period decrease by a light-time effect (LITE) caused by the presence of one or two other bodies, respectively. Dumitrescu (1973b, 1974) analyzed photometric LCs of RT And obtained in 1971 (Dumitrescu, 1973a) and found a slightly eccentric orbit with $e = 0.08$. He explained some characteristics of the LC by random mass loss from the primary component almost filling the corresponding Roche lobe and a hot spot on the secondary component. Milano et al. (1981) analyzed 10 available photoelectric LCs obtained up to 1978, derived mean photometric elements and proposed a “migration wave” caused by the spots with a period of about 22 years equal to the magnetic activity cycle. Zeilik et al. (1989a) explained the photometric distortion waves in the LCs by dark, circular starspots. Since RT And is quite bright, it was one of the targets of the

Hipparcos astrometric mission. The resulting parallax $\pi = 13.3 \pm 1.1$ mas (Popper, 1998) corresponding to the distance $d = 75 \pm 6$ pc is a crucial test of the correct determination of absolute parameters of RT And and constitutes the main impetus for the present study.

3.1 The orbital period analysis

For the analysis of period changes we have gathered all available photographic and photoelectric minima times from literature. Minima times determined from visual estimates were omitted. Older times of minima were taken from Williamon (1974), Bakos & Tremko (1981) and Rovithis-Livaniou et al. (1994). Recent minima times were taken from IBVS. The weights 1 and 5 were accepted for the minima times determined from the photographic and photoelectric observations, respectively. The averages calculated from minima times in different passbands were used. Altogether 169 minima times (41 photographic and 128 photoelectric) listed in Table 3 were used for further analysis. Two photographic and three photoelectric minima times deviating too much from the general trend were omitted. They are listed under the line at the end of compilation of the photographic and photoelectric minima. Detected differences in the relative position of the secondary minima with respect to the expected photometric phase 0.5 were explained by an eccentric orbit. Milano (1981) found them to be highly variable and concluded that eccentricity is only the result of numerical artifice. On the other hand, Zeilik et al. (1989a) found from the LC analysis small eccentricity $e = 0.026 \pm 0.013$. The displacement of the secondary minimum can be calculated in the first approximation (for small eccentricities, and inclination $i = 90$) by the well known relation:

$$\Delta T = \text{Min II} - \text{Min I} - P/2 = 2Pe \cos \omega / \pi$$

where Min II and Min I are times of consecutive secondary and primary minima, respectively. Parameter ω is the length of the periastron of the primary component. The displacement vanishes for $\omega = 90$ and 270 . Before the beginning of the spectroscopic observations analyzed in Sect. 4 only five secondary minima times were published. Ten secondary minima times fall within the range of the spectroscopic observations (1984-94). If we accept the spectroscopic elements: $e = 0.011 \pm 0.004$ and $\omega = 73 \pm 26$ (Table 6), the relation (1) provides $\Delta T = 0.0012 \pm 0.0018$ days. The scatter of the minimum times is about 0.003 days.

3.3. Simultaneous solution of the composite light

and radial velocity curves In most previous LC analyses of RT And (Zeilik, 1989a; Heckert, 1995, 1996, 1998; Ar'evalo et al., 1995) the LCs in different passbands were treated separately leading to different geometrical elements for each passband. The mass ratio was usually either assumed from spectroscopy or both components were approximated by spheres. Since we had at our disposal all RVs and LCs in 7 passbands, we decided to take advantage of the simultaneous LC and RV curve fitting (see Wilson, 1979) and multifrequency analysis. The B,V,R and KLCs and RVs were analyzed using the synthetic LCs and the differential corrections code developed by Wilson & Devinney (1971) (W&D). We have used the 1992 version (Wilson, 1992) of his program. The particular numbers of individual photometric observations coming into one normal point were used as weights. The RV data were not weighted individually. For each LC and RV curve the values of were carefully evaluated as described by Wilson (1979). The initial values of photometric and spectroscopic parameters of RT And were taken from Wang & Lu (1993). Mode 2 of the W&D code appropriate for detached binaries was employed assuming synchronous rotation and zero eccentricity. For the computation of

luminosities we have used the approximate atmospheric models option of the W&D program (Carbon-Gingerich atmospheres). Coefficients of gravity darkening $g_1 = g_2 = 0.32$ (Lucy, 1967) and bolometric albedo $A_1 = A_2 = 0.5$ (e.g., Rucinski, 1969) were fixed as appropriate for the convective envelopes. The limb darkening coefficients were interpolated from Table 1 of Al-Naimiy (1978). The spectral type - effective temperature calibrations differ markedly: Johnson (1966) gives for F8V $T_{\text{eff}} = 6000$ K and for G0V $T_{\text{eff}} = 5900$ K, while Lang (1992) gives $T_{\text{eff}} = 6200$ K and $T_{\text{eff}} = 6030$ K. Therefore we have fixed the mean temperature of the primary component at two boundary values 6200 and 5900 K. Ar'evalo et al. (1995) found that the infrared LCs can be fitted almost equally well by two sets of photometric parameters for $i = 82^\circ$ and $i = 87^\circ$. The analysis of the eclipse morphology, evolutionary models prediction as well as 2 favour the high inclination solution. These solutions differ mainly in the ratio of radii of the primary and secondary component. To validate all possibilities we have performed four solutions – two for high inclination and two for low inclination. In each case we have run the differential correction code as long as output corrections were smaller than the errors of the elements. The resulting geometric elements do not differ significantly for the solutions with different temperatures. Therefore, we present only the lower temperature solution in Table 8. Fits corresponding to the high and low inclination solution differ only slightly (Fig. 8). The most marked difference is the constant-light phase during the secondary minimum due to the total eclipse of the secondary component. For the lower inclination the eclipses are partial. The weighted sum of squares of the residuals favors the high inclination solution. We have also checked the possibility of a small orbital eccentricity by analysis of the mean LCs. This approach is justified.

Table (1) : The light curve fit parameters for RT And

Parameter	Star1	Star2
Mass Ratio (M2/ M1)	0.970000	
Surface Potential Ω	4.310000	4.140000
Temperature	9800.00	9790.00
Gravity Darkening	0.320	0.320
Limb Darkening	0.418	0.418
Reflection	2.300	2.400
Inclination	82.600	

Where Ω_1 and Ω_2 = surface potential of the primary and the secondary components, C_1 and C_2 = potential of the primary and the secondary components, f_1, f_2 = Fillout of the primary and the secondary components, L_1, L_2 = Absolute parameter of components in units of solar Luminosity

Table (2): The output parameters for RT And

$\Omega_1 = 4.310000$	$\Omega_2 = 4.140000$
$\Omega_{inner} = 3.701085$	$\Omega_{outer} = 3.171423$
$C_1 = 3.901118$	$C_2 = 3.901118$
$C_{inner} = 3.901907$	$C_{outer} = 3.559723$
$f_1 = 0.002308$	$f_2 = 0.002308$
Lagrangian $L_1 = 0.595817$	Lagrangian $L_2 = 1.540608$
$r_1(\text{back}) = 0.491415$	$r_2(\text{back}) = 0.325065$
$r_1(\text{side}) = 0.464740$	$r_2(\text{side}) = 0.292304$
$r_1(\text{pole}) = 0.435204$	$r_2(\text{pole}) = 0.280426$
Surface area 1 = 2.733718	Surface area 2 = 1.145661
Mean radius 1 = 0.463786	Mean radius 2 = 0.299265

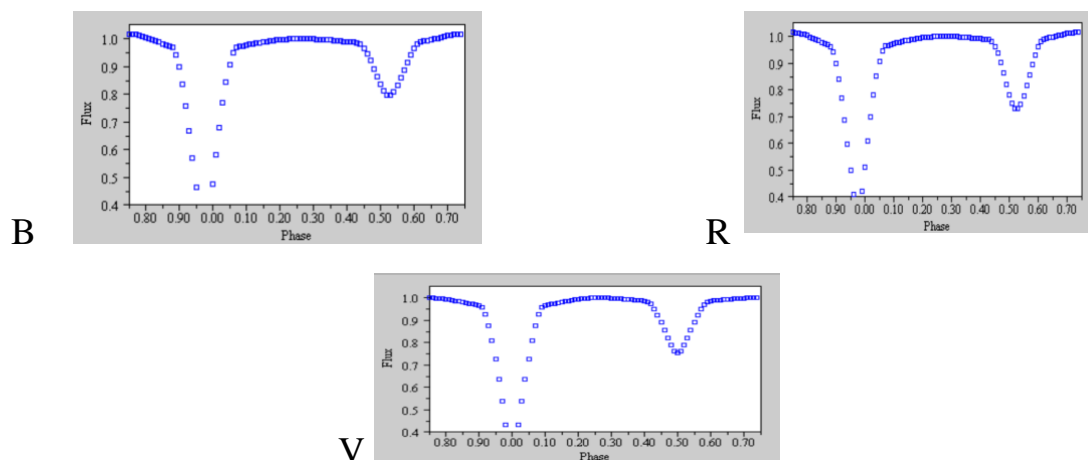


Figure (1-1): Light curve fitting for B, V and R Filter for RT And .

Also we can calculate absolute parameters for stars by using equation(2.17 to 2.22)

Table (3): Absolute parameter (in solar units)of the systems for short period binary star

Star	R1	R2	M1	M2	L1	L2	Type	Refrence
RT And	2.16	1.3496	0.5076	0.4924	43	46	F	Present work
RT And	2.3	2.4	2.7	2.76	44	47	F	A. Liakos 2012

5.2 Bolometric Magnitudes- $M_{bol1,2}$:

Table (4): Adapted auxiliary parameters for active short period binary system.

Star	x_1	x_2	g_1	g_2	E_1	E_2
RT And B	0.492	0.493	0.3019	0.3022	4.5244	4.5204
V	0.418	0.419	0.2933	0.2935	4.6577	4.6535
R	0.353	0.354	0.2860	0.2863	4.7762	4.7718

5.3 Age- Mass relationship for CA binaries of stars:

The Age- Mass can be determined using Equation (12), for this purpose programs handled using Mat lab program. The Table (5) represents the present work parameters regarding the age-mass relation.

Table (5): The age-mass relation for other investigation:

Star	Primary log Age	Secondary log Age
RT And	109.0367	110.2542

.4 The Life Time:

The Life time can be determined using Equation (13), for this purpose Mat lab programs handled. The table (6) represents the present results relating life time of short period binary systems.

Table (6): Lifetime of short period binary systems

Star	$t_1/t_{\text{sun}} * 10^{83}$	$t_2/t_{\text{sun}} * 10^{83}$
RT And	4.0133	4.0133

6. Geometry of Roche Loop:

The unique form of the Roche lobe relies upon at the mass ratio $q = M_1/M_2$, and should be evaluated numerically. However, for plenty functions it's miles beneficial to approximate the Roche lobe as a sphere of the identical volume. An approximate system for the radius of this sphere is

$$r_1/A = \max [f_1, f_2], \text{ for } 0 < q < 20 \dots \dots \dots (18)$$

Where $f_1 = 0.38 + 0.2 \log (q)$ and $f_2 = 0.46224 (q/1+q)^{1/3}$. Function f_1 is extra than f_2 for $q > 0.5228$. The duration A is the orbital separation of the machine and r_1 is the radius of the sector whose extent approximates the Roche lobe of mass M_1 . This components is correct inside to approximately 2%. (Paczynski, B. (1971) Another approximate components became possible Eggleton's method and reads as follows:

$$r_1/A = 0.49 q^{2/3} / 0.6 q^{2/3} + \ln (1+q^{1/3}) \dots \dots \dots (19)$$

This formula gives results up to 1% accuracy over the entire range of the mass ratio q (Eggleton, P. P. (1 May 1983) . The fig (6) show The shape of the spotted model of the AD And binary system at different phases.

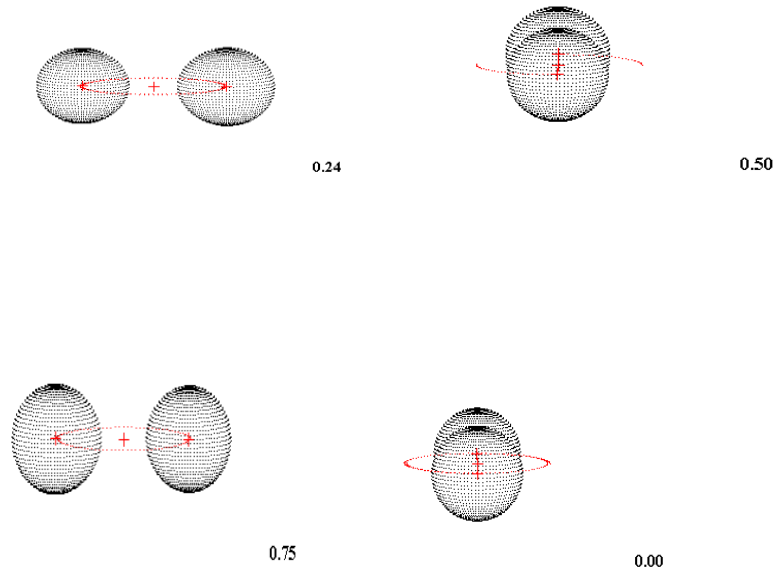


Figure (6): Shows the shape of the spotted model of RT And binary star at different phases.

7 First Contact Angle:

The First contact angle can be determined using Eqs. (14) to (16), for this purpose programs handled using Mat lab program. The Table (8) represents the present first contact angle and type of eclipse.

Table (8): First contact angle and type of eclipse.

Star	θ_1	a	C_o	Type of eclipse
RT And	0.2271	2.5175	0.7454	F5V

1.8 Empirical Relationship between CI , M_{bol} and T_{eff} :

The Empirical Relationship between CI , M_{bol} and T_{eff} can be determined using Eqs. (16) to (22), for this purpose programs handled using Matlab program. The Table (9) represents the present empirical values for primary and secondary stars of the binary system.

Table (9): Empirical values for present work.

Star	Component	BC= $M_{bol}-M_v$	CI= B-V	M_{bol}	M_v
RT And	Primary	0.1749	25.6169	82.2777	82.1028
	Secondary	-0.1734	25.0349	83.2751	83.1017

5 RESULTS AND DISCUSSION

In Table 2 we list our results from fitting the O – C diagram for RT And together with early published results. Parameters of our solution are almost the same as in previous papers, except for the orbital period P3 of the third body. It is about 2 years shorter (12.1 yr, in contrast to 14.3 yr) than in other solutions. This difference can be explained by the fact that we have used a much longer time interval for an analysis. Liao & Qian (2009) and Liakos et al. (2012) used only minima times from photoelectric and CCD observations and neglected all O – C points obtained before 1990 because of their poorer quality. We also used these older photographic and visual observations even with smaller weight. Moreover, the last CCD minima times cover the full cycle of O – C variations (see Fig. 2). We also detected a secular period change (parameter Q) not mentioned by other authors. The period change corresponds to increase of the period $dP/dt = 1.06(94) \times 10^{-4} \text{ s yr}^{-1}$ and should be connected with mass transfer from the secondary component to the primary one and/or with the Applegate effect (Applegate 1992), but this is not in agreement with a detached configuration of the system (Liakos et al. 2012). It is necessary to note that the relative statistical error of Q is almost 90%, which degrades its significance. We cannot confirm or disprove the secular period changes and only future observations can resolve this problem. Our solution implies a minimal 3rd body mass (for $i_3 = 90^\circ$) of $\sim 2.33 M_\odot$, using absolute parameters from Liakos et al. (2012). This would indicate that the third light contributes about 15% to the total

luminosity of the system, but the third light resulting from light curve analysis (Liakos et al. 2012) is about 3%. This difference can be explained with the assumption that the 3rd star is actually a binary system with two solar-mass components as mentioned by Liakos et al. (2012).

6. References:

Applegate, J.H., 1992. ApJ 385, 621.

Asplund, M., Grevesse, N., Sauval, A. J., & Scott, P. 2009, ARA&A, 47, 481.

Borkovits, T., Hegedüs, T., 1996. A&AS 120, 63.

Briede, A., 1949. Peremennye Zvezdy 6, 283.

Barrado D., Femàndez-Figueroa M. J., Montesinos B., De Castro E., 1994, A&A, 290, 137

Budding, E. 1984, Bulletin d'Information du Centre de Donnees Stellaires, 27, 91.

Claria, Juan J.; Piatti, Andres E.; Lapasset, Emilio (May 1994). "A revised effective-temperature calibration for the DDO photometric system". *Publications of the Astronomical Society of the Pacific*. 106:436.

Eggleton, P. P. (1 May 1983). "Approximations to the radii of Roche lobes". *The Astrophysical Journal*. 268: 368.

Frieboes-Conde, H., Herczeg, T., 1973. A&AS 12, 1.

Gradients of Open Clusters". *Astronomy and Astrophysics*. 147.

Gaposchkin, S., 1932. Ver. Berlin Babelsberg 9, 5.

Gajdos̃, P., & Parimucha, S̃ . 2018, submitted to A&C.

Giuricin, G., Mardirossian, F., 1981. A&AS 45, 499.

Guthnick, P., & Preger, R. 1927, *Kleine Veroeffentlichungen der Universitaetssternwarte zu Berlin Babelsberg*, 1, 4.1.

Hill, G., Hilditch, R.W., Younger, F., Fisher, W.A., 1975. *Mem. Roy. Astron. Soc.* 79, 131.

Johnson, H. L.; Morgan, W. W. (May 1953). "Fundamental stellar photometry for standards of spectral type on the revised system of the Yerkes spectral atlas". *The Astrophysical Journal*. 117:313.

J. L. Puget; J. Heyvaerts (1980). "Population III stars and the shape of the cosmological black body radiation". *Astronomy and Astrophysics*. 83 (3): L10–L12.

Kopal, Z., 1959. *Close Binary Systems*. Chapman & Hall, London.

Kopal Z., "Language of the Stars". D. Reidel Publishing Company, Dordrecht, London, (1979).

Koch, R.H., Plavec, M., Wood, F.B., 1970. *Publ. Univ. Pennsylvania, Astron. Ser.*, No. 10.

Kreiner, J.M., Kim, C.H., Nha, I.S., 2001. *An Atlas of O–C diagrams of eclipsing binary star*. Wydawnictwo Naukowe Akademii Pedagogicznej, Cracow, Poland. *Recipes: The Art of Scientific Computing* (3rd Edition, Cambridge: Cambridge Univ.

Liao, W. & Qian, S. 2009, *New A*, 14, 249

Liakos, A., Zasche, P., & Niarchos, P. 2011, *New Astron.*, 16, 530

Liakos A., Niarchos P. & Budding E. 2012, *A&A*, 539, 129

Matteucci, Francesca (2001). *Astrophysics and Space Science Library*. Vol. 253. Springer Science & Business Media. p. 7

M., Cameron, L. (June 1985). "Metallicities and Distances of Galactic Clusters as Determined from UBV Data Part Three Ages and Abundance Paschke Anton., 1997. *BBSAG Bull.*, No. 114.

Press, W. H., Teukolsky, S. A., Vetterling, W. T., & Flannery, B. P. 2007, *Numerical*

Paczynski, B. (1971). "Evolutionary Processes in Close Binary Systems". *Annual Review of Astronomy and Astrophysics*. 9:183-208.

Qian, S.B., Liu, Q.Y., Tan, W.L., 2000. ApSS 274, 859.

Rucinski, S.M. 1966, Acta Astron., 16, 307

Wood, D.B., 1972. A computer program for modeling non-spherical eclipsing binary systems. Goddard Space Flight Center, Greenbelt, Maryland, U.S.A. Wallerstein, George; Carlson, Maurice (September 1960).

"Letter to the Editor: on the Ultraviolet Excess in G Dwarfs". The Astrophysical Journal. 132:

Whitney, B.S., 1957. AJ 62, 37. Wilson, R.E., 1990. ApJ 356, 613.

Zasche, P., Liakos, A., Niarchos, P., et al. 2009, New A, 14, 121.